(12) UK Patent Application (19) GB (11) 2 317 446 (13) A

(43) Date of A Publication 25.03.1998

(21) Application No 9619690.2

(22) Date of Filing 20.09.1996

(51) INT CL[6]
G01J 3/45

(52) UK CL (Edition P)
G1A AA6 ACDT AG18 AR6 AR7 AT24

(56) Documents Cited
None

(58) Field of Search
UK CL (Edition O) G1A ACDT AHSL
INT CL[6] G01J 3/45 3/453
Online: WPI

(71) Applicant(s)
NPL Management Limited

(Incorporated in the United Kingdom)

Serco plc, Queens Road, TEDDINGTON, Middlesex, TW11 OLW, United Kingdom

(72) Inventor(s)
David Henry Nettleton

(74) Agent and/or Address for Service
Graham Jones & Company
77 Beaconsfield Road, Blackheath, LONDON, SE3 7LG, United Kingdom

(54) Fourier transform spectrometer

(57) Spectrometer apparatus comprising a dispersive spectrometer for example a prism, which operates to disperse an incoming spectrum into a plurality of spectral bands extending in a first direction, a Fourier transform spectrometer which generates in a second direction (which may be at right angles to the first direction) an interferogram of each of the spectral bands, and a 2-dimensional detector array for example a 1024 x 1024 pixel CCD. The detector array may be positioned behind an array of slots.

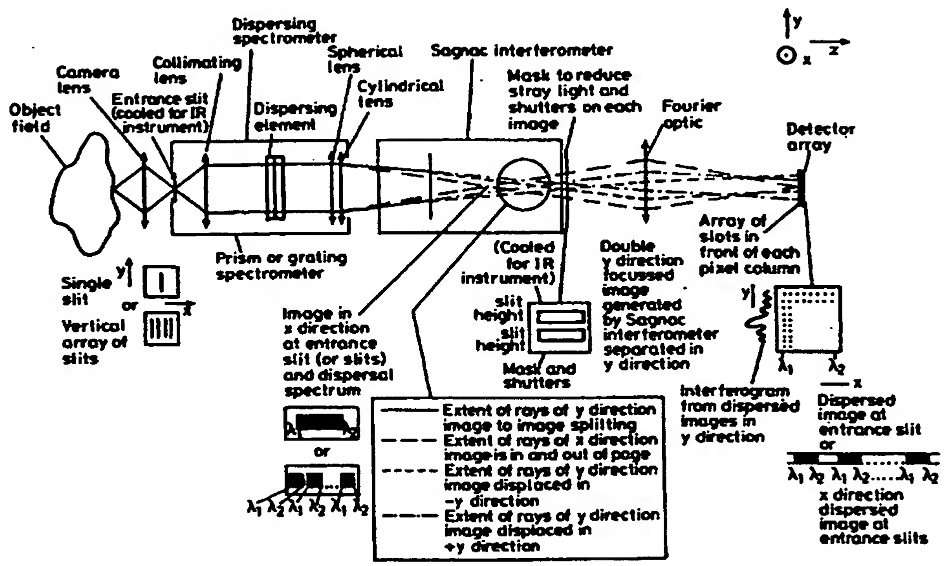

Figure 3 Schematic diagram of 2 dimensional detector array high resolution spectrometer.
Lenses could be mirrors. Image positions could vary, only example given.
In practice components change direction of central ray, not shown

At least one drawing originally filed was informal and the print reproduced here is taken from a later filed formal copy.

GB 2 317 446 A

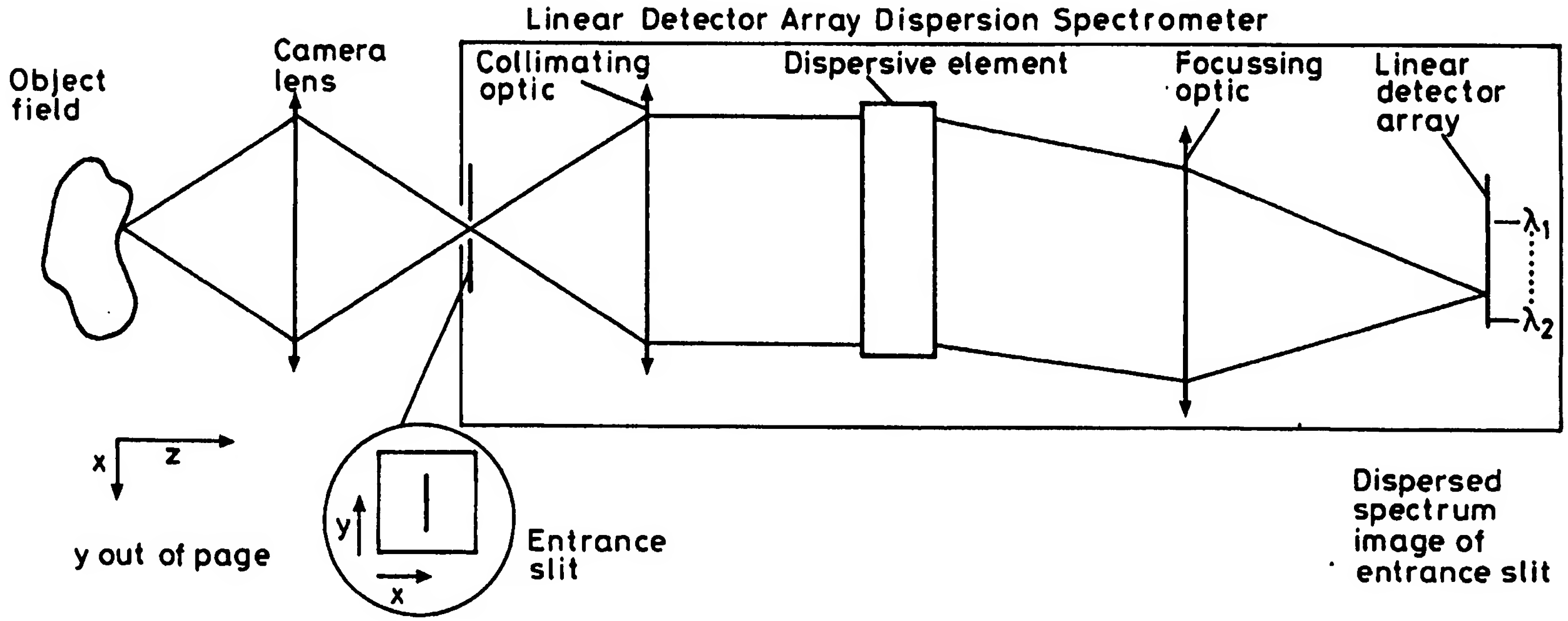

Figure 1 Dispersive Spectrometer

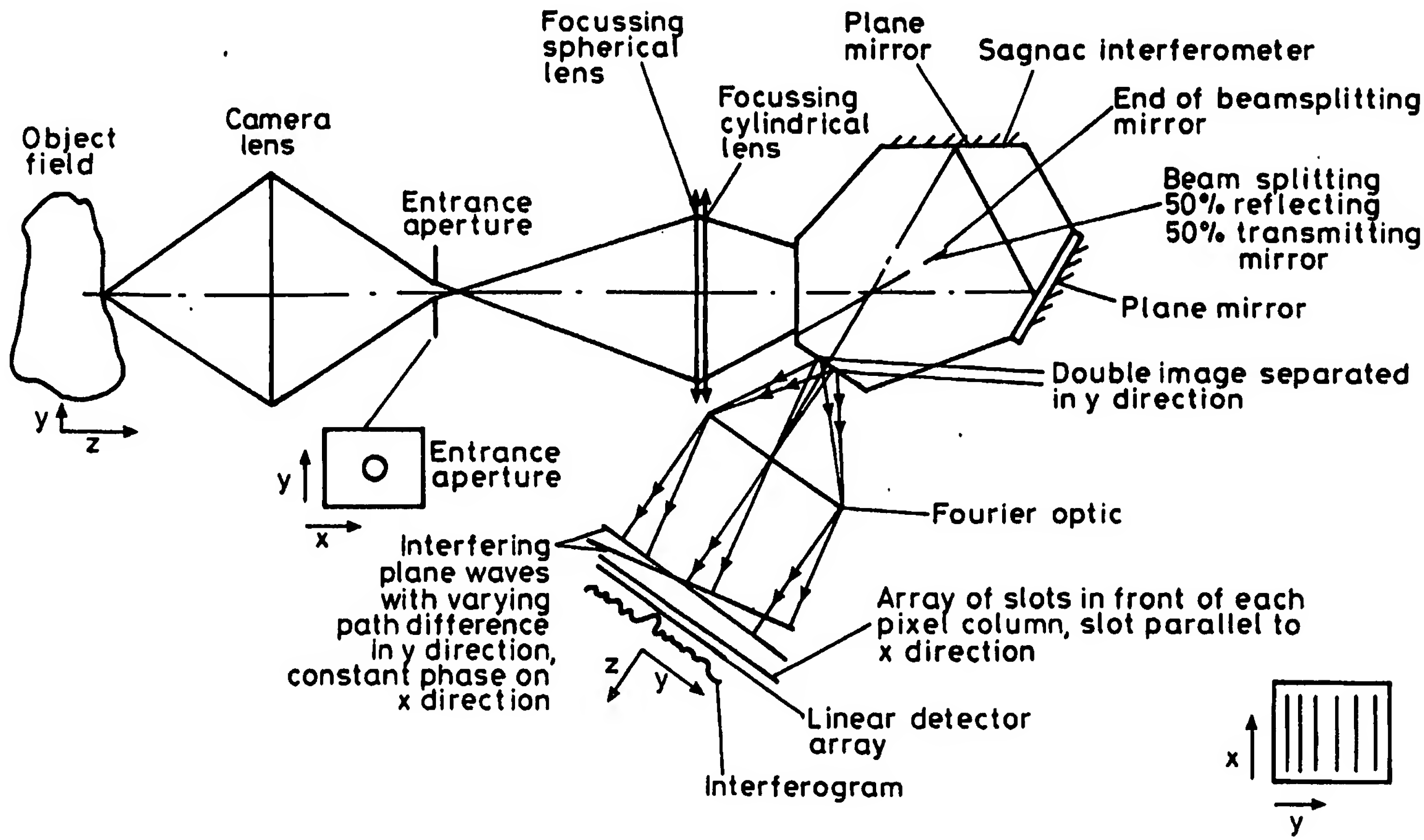

Figure 2 Sagnac Interferometer Fourier Transform Spectrometer

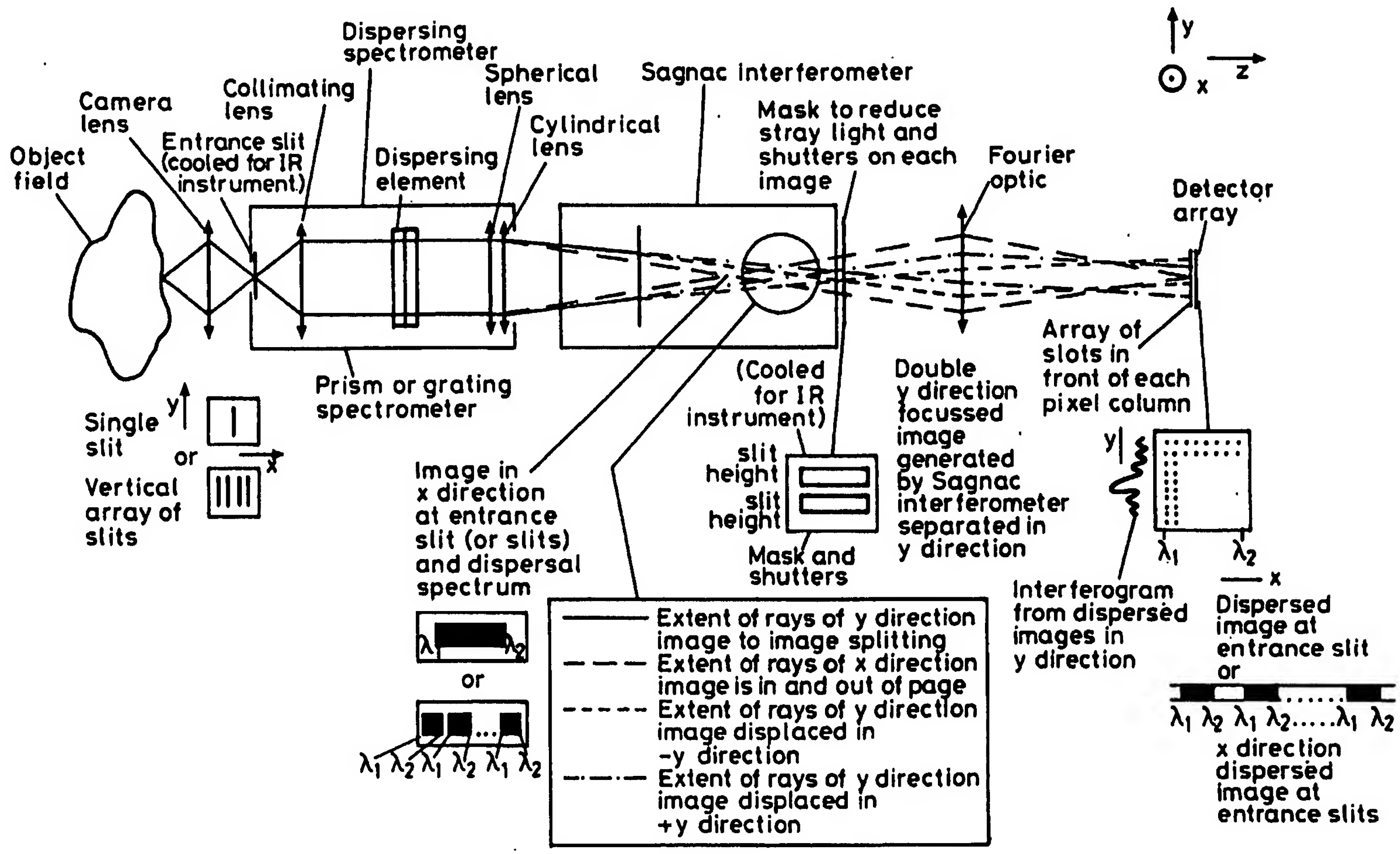

Figure 3 Schematic diagram of 2 dimensional detector array high resolution spectrometer. Lenses could be mirrors. Image positions could vary, only example given. In practice components change direction of central ray, not shown

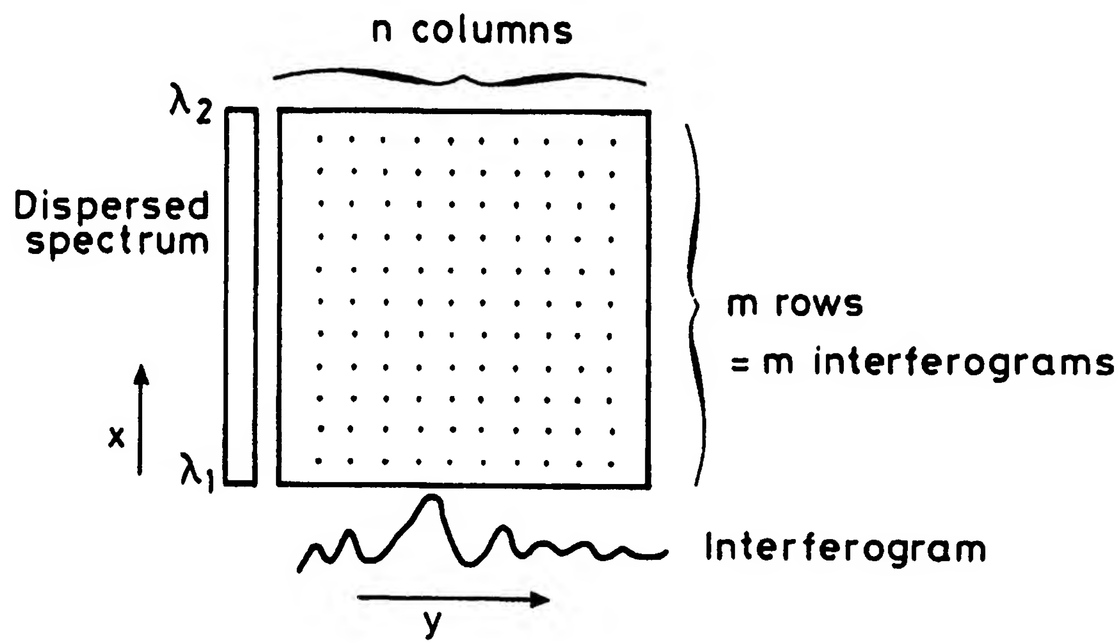

Figure 4 Detector array
Each of m rows has different interferogram
for $\Delta\lambda_m$ ($\Delta\lambda_1$, $\Delta\lambda_2$ ..... $\Delta\lambda_m$)

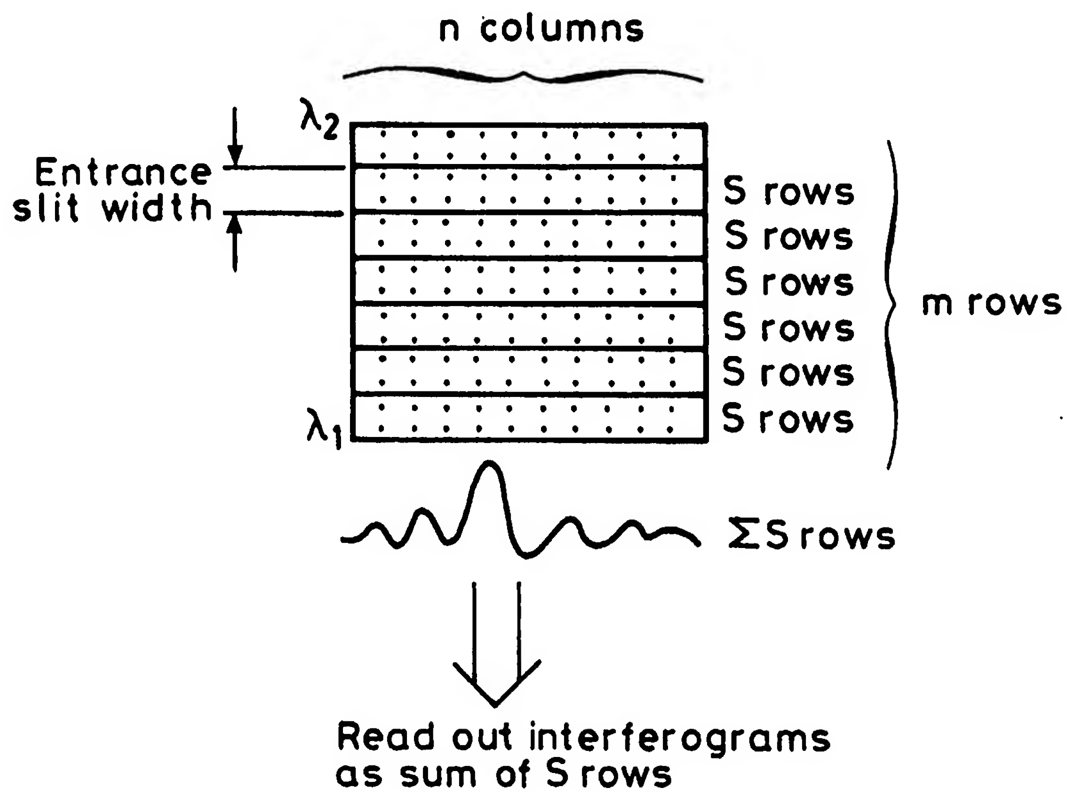

Figure 5 Detector array showing 'binning' rows to increase throughput at reduced resolution

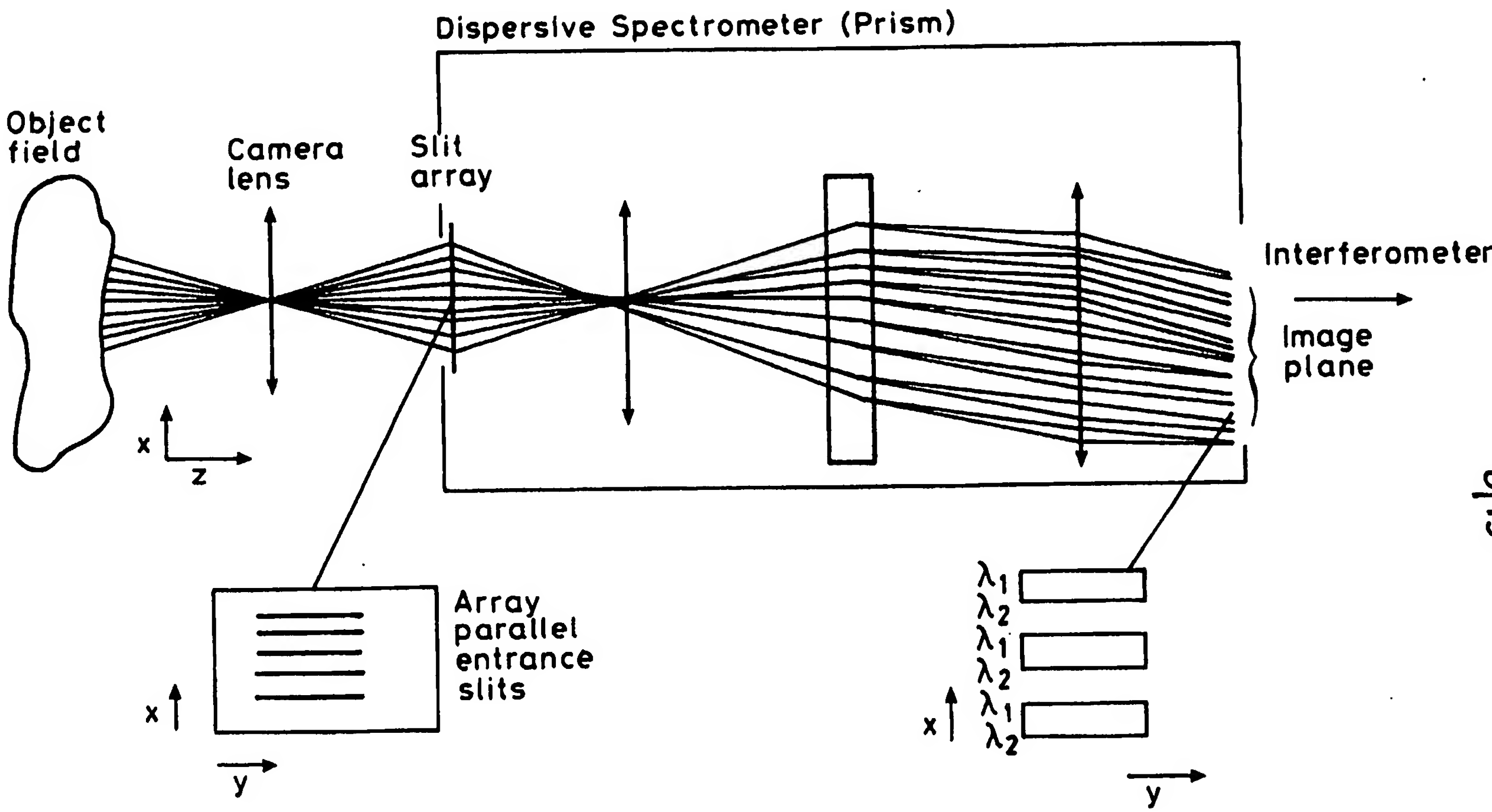

Figure 6 Array of parallel entrance slits give spatial resolution of object field in x direction

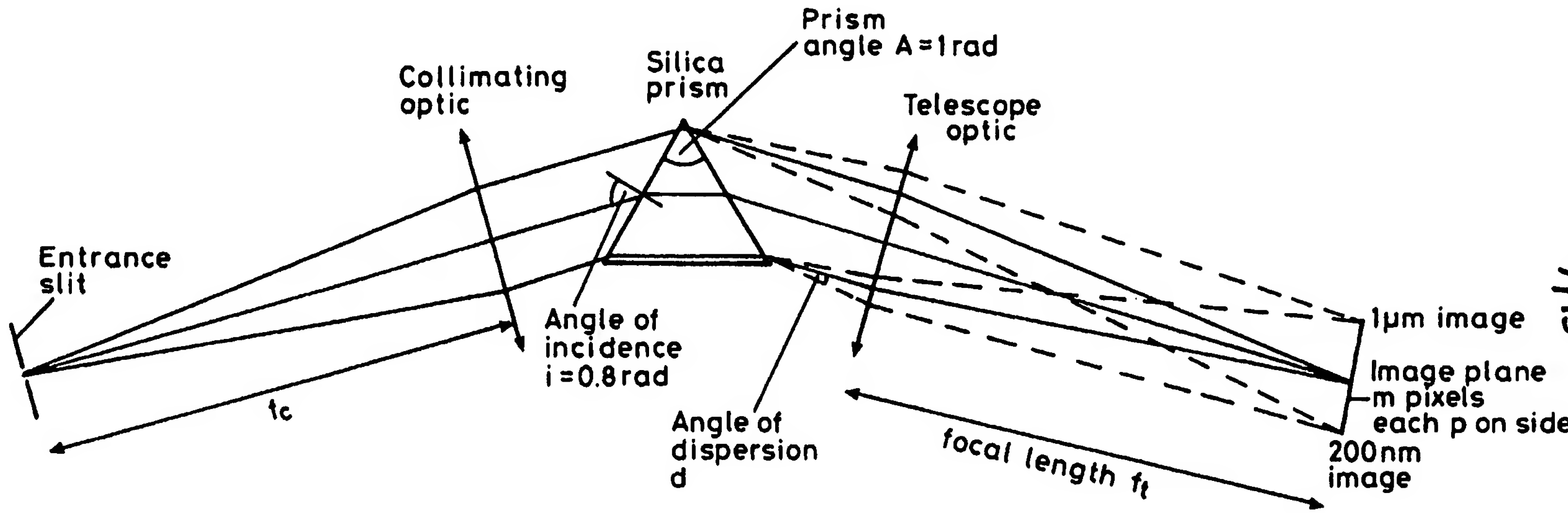

Figure 7 Schematic of silica prism spectrometer of Example 1

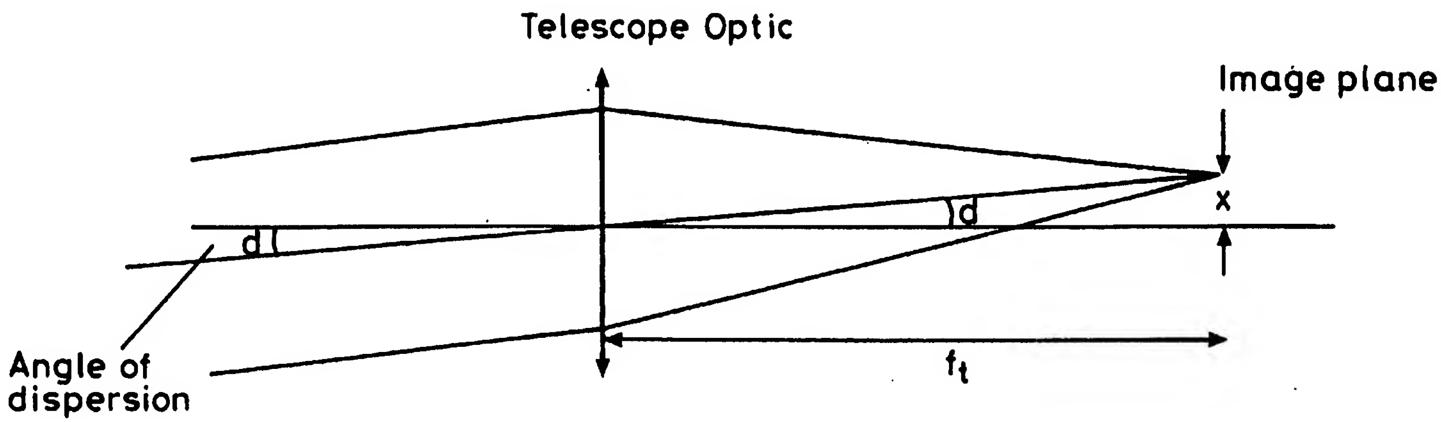

Figure 8 Figure showing dispersion

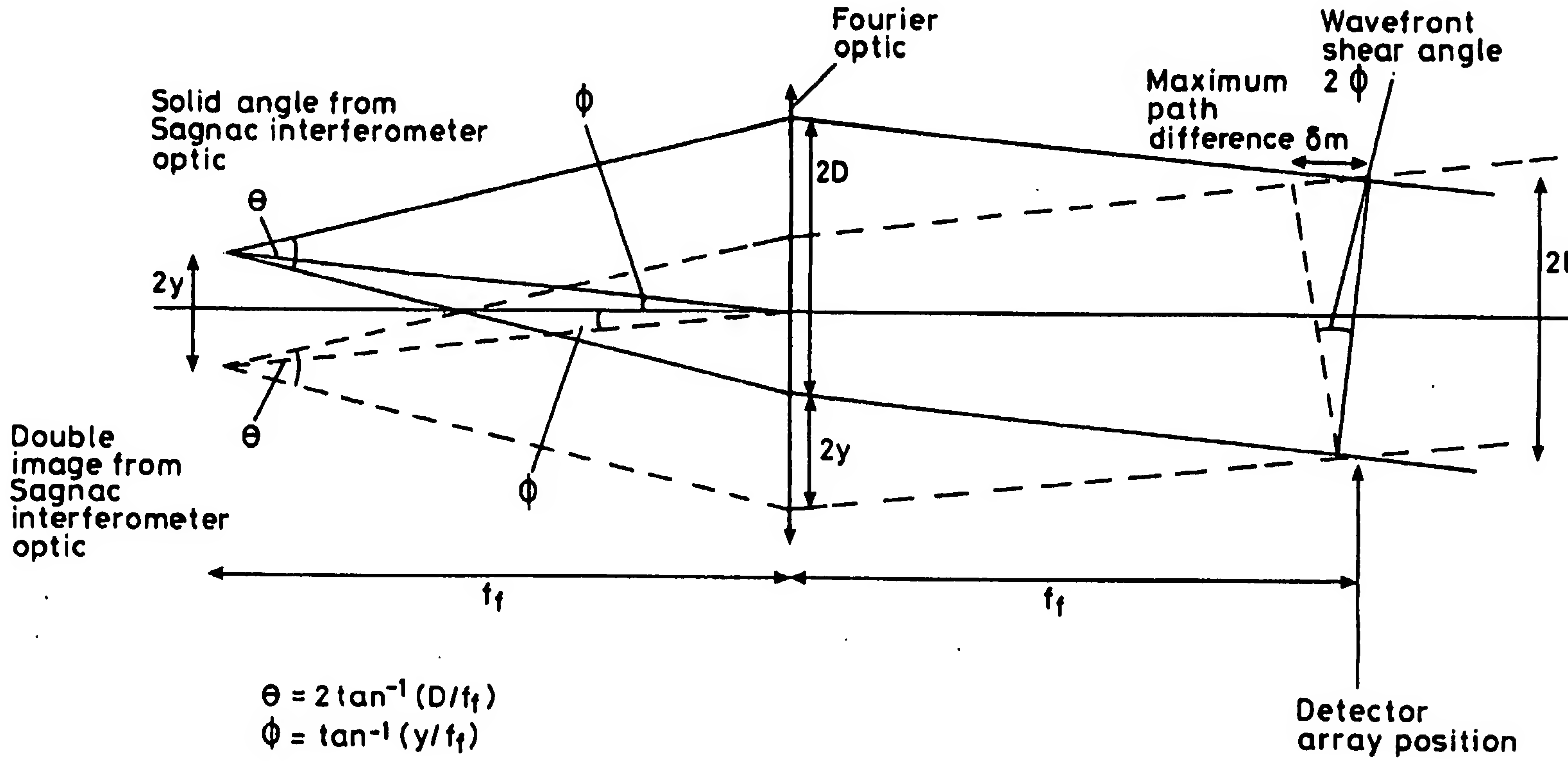

$\theta = 2\tan^{-1}(D/f_f)$
$\phi = \tan^{-1}(y/f_f)$

Figure 9 Figure showing Fourier optic

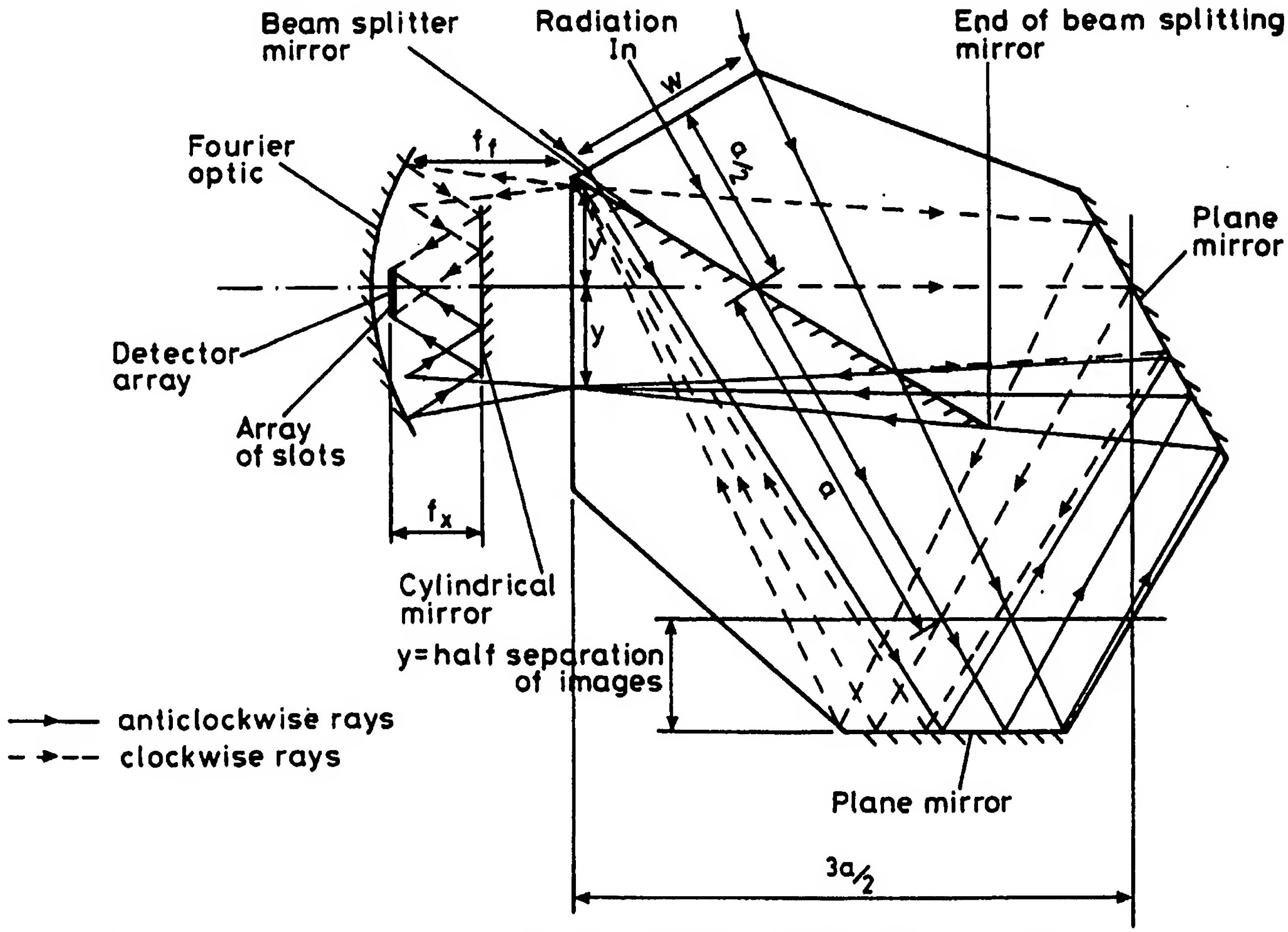

Figure 10 Figure showing silica Sagnac interferometer (1/2 full size) described in Example 1

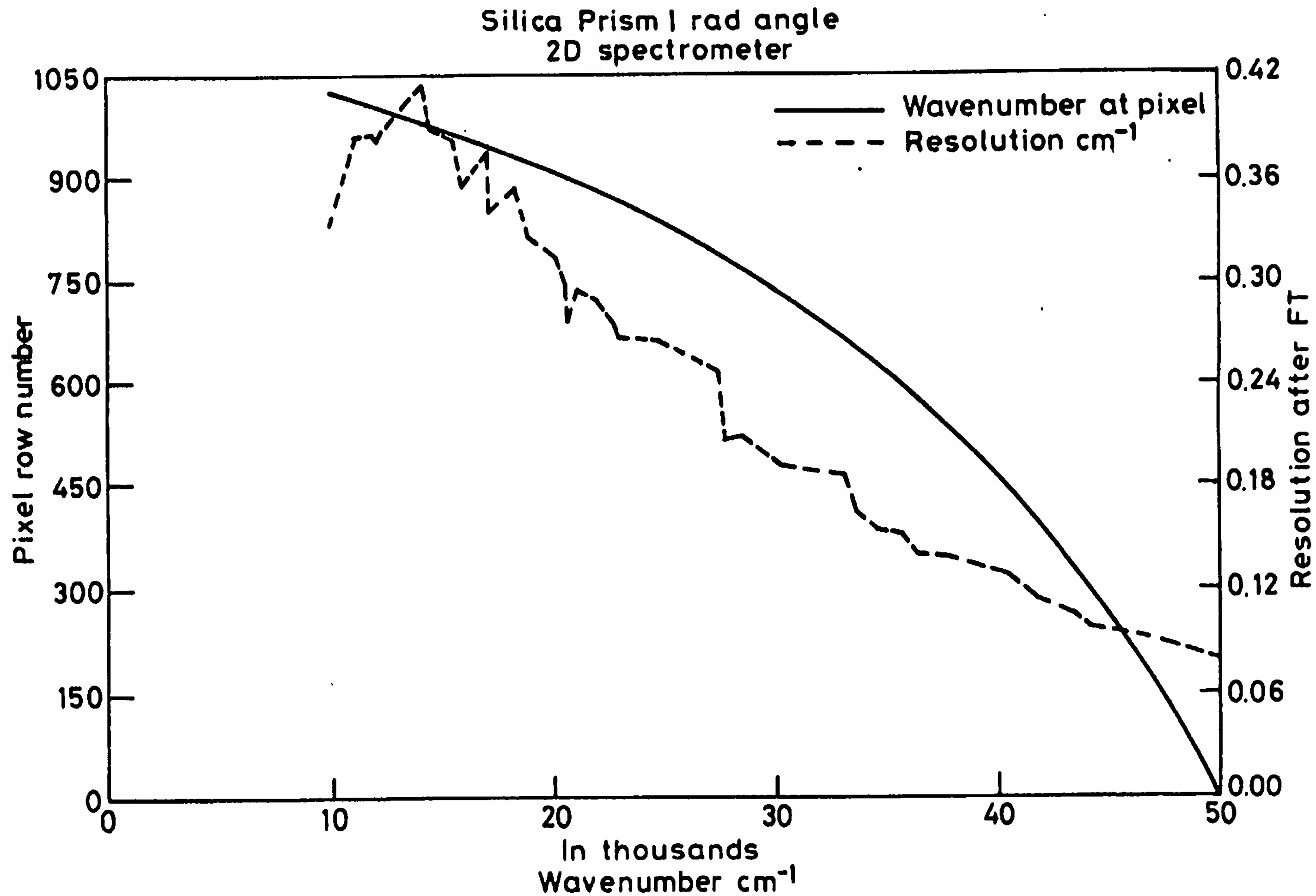
Silica Prism I rad angle
2D spectrometer
Wavenumber at pixel
Resolution cm⁻¹
Pixel row number
1050
900
750
600
450
300
150
0
Resolution after FT
0.42
0.36
0.30
0.24
0.18
0.12
0.06
0.00
0
10
20
30
40
50
In thousands
Wavenumber cm⁻¹

Figure 11

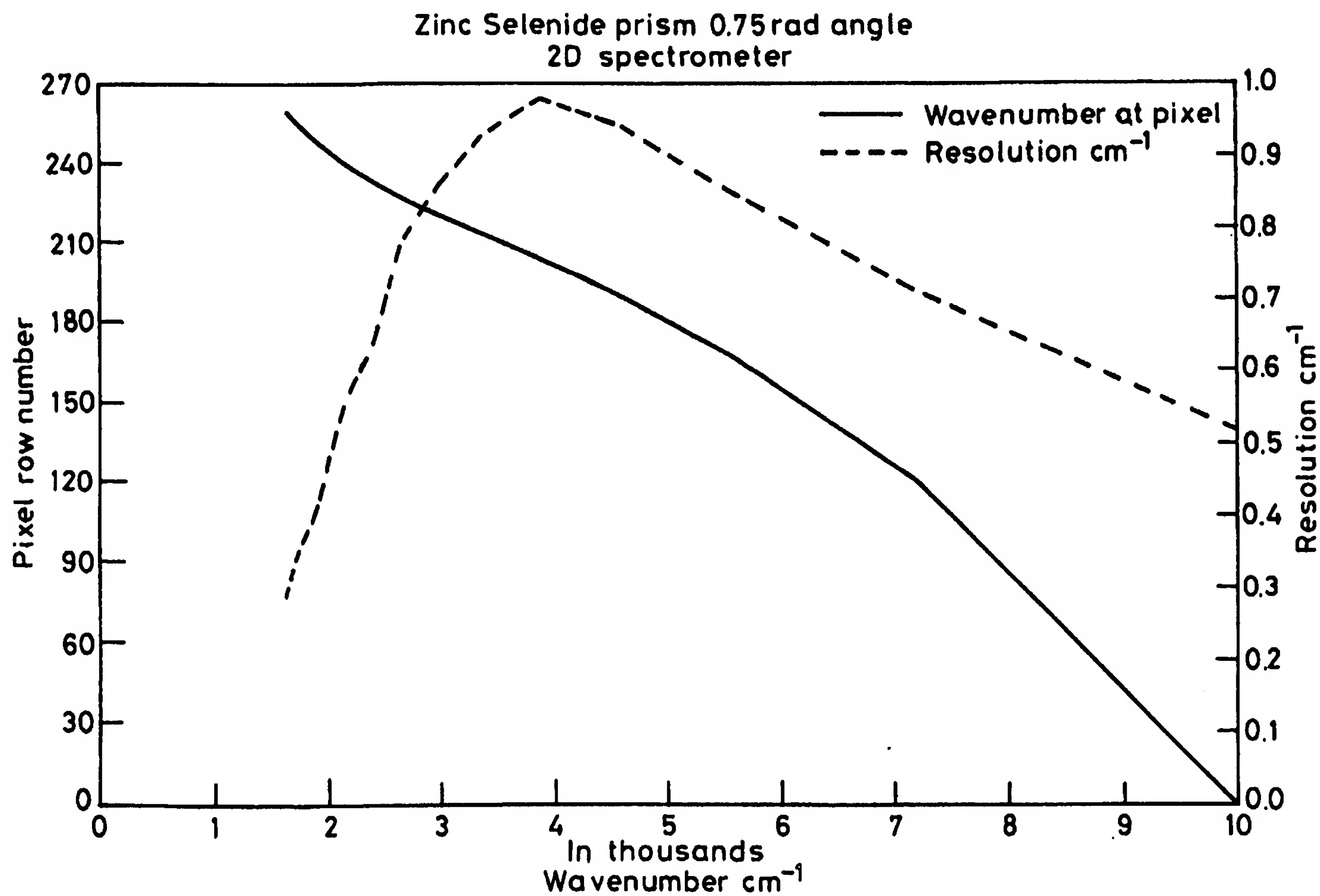
Zinc Selenide prism 0.75 rad angle
2D spectrometer
Wavenumber at pixel
Resolution cm^{-1}
Pixel row number
270
240
210
180
150
120
90
60
30
0
Resolution cm^{-1}
1.0
0.9
0.8
0.7
0.6
0.5
0.4
0.3
0.2
0.1
0.0
0
1
2
3
4
5
6
7
8
9
10
In thousands
Wavenumber cm^{-1}

Figure 12

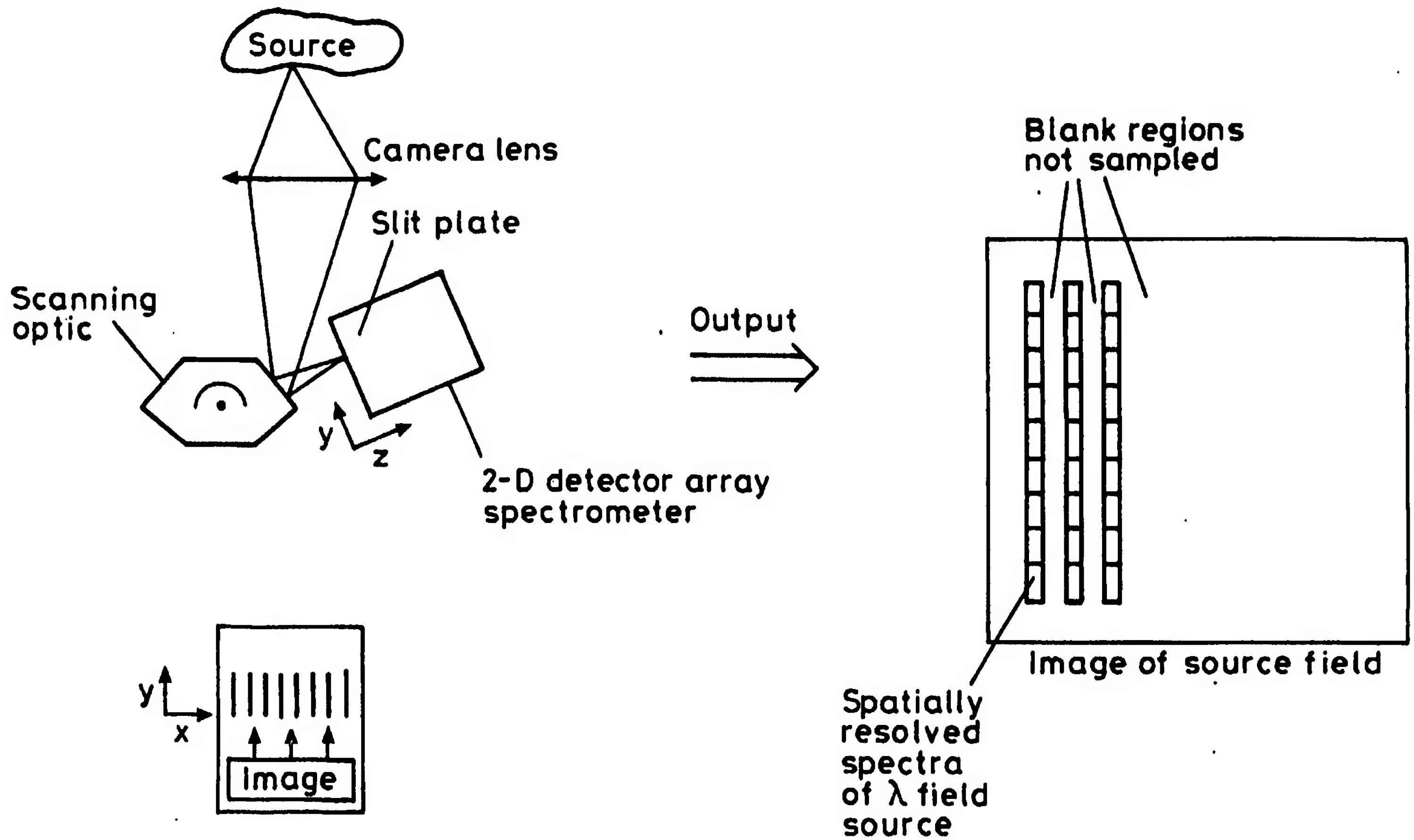

Figure 13 Schematic of system to generate 2-D spatially resolved spectra of source

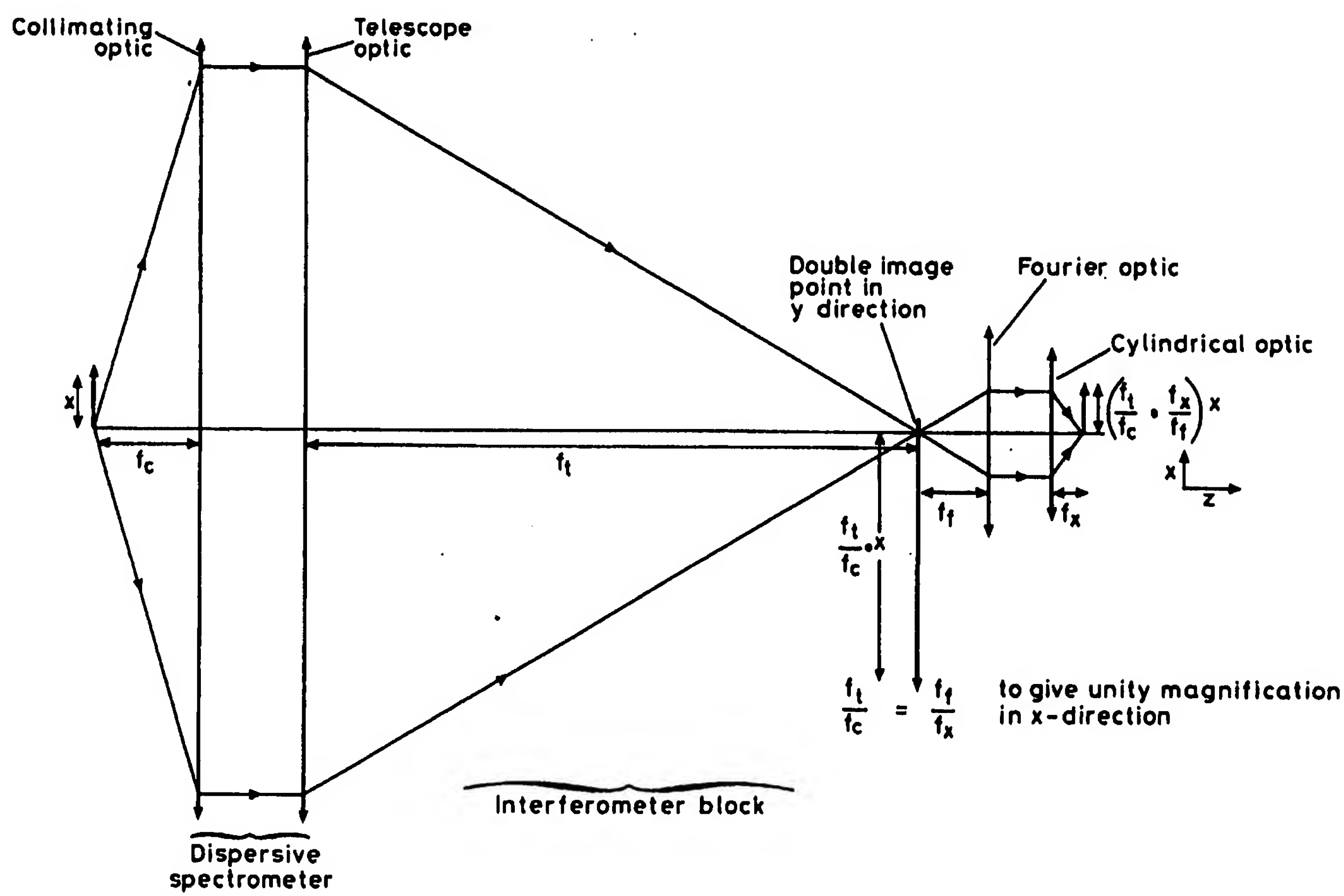

Figure 14 Schematic of imaging system in x direction

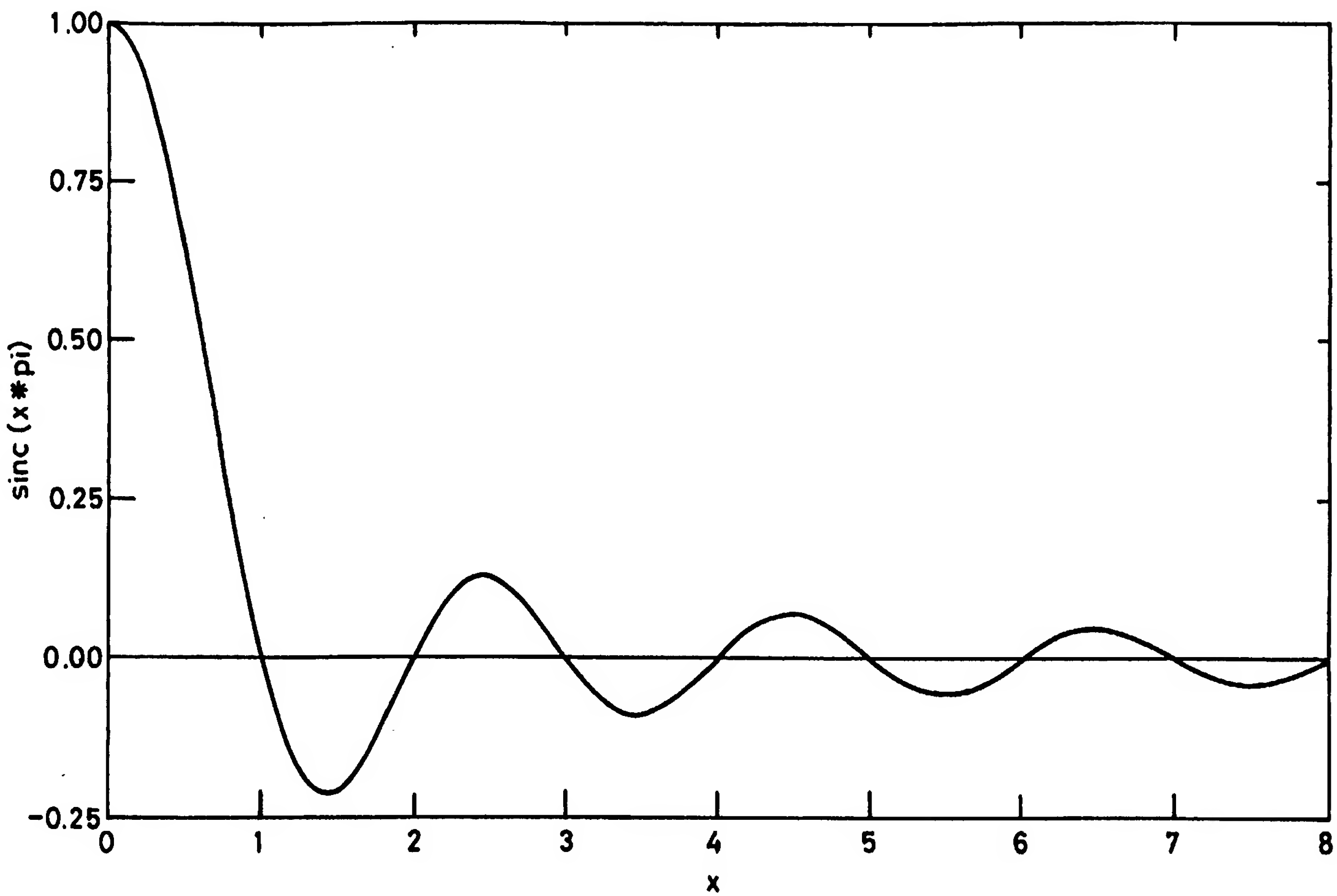

Figure 15 Plot of a $\frac{\sin(x)}{x}$ = sinc (x)

2317446

SPECTROMETER APPARATUS

This invention relates to spectrometer apparatus and, more especially, this invention relates to spectrometer apparatus having a high resolution over a wide spectral region capability.

The wide availability of multi-element detector arrays has led to the development of spectrometer apparatus that is able to record a complete spectrum from a source all at the same time. This is in contrast with spectrometer apparatus that scans an optical element over an angle or distance to record the spectrum over the scanning time. The most common type of spectrometer apparatus that records a complete spectrum from a source all at the same time is a linear detector array dispersion spectrometer. A less common but still known type of apparatus is a spatially modulated Fourier transform spectrometer which also uses linear detector arrays.

The resolution of the known linear detector array dispersion spectrometers and also of the Fourier transform spectrometers is usually limited by the number of detector elements (pixels) in the linear array. Typically, the resolution of the spectrometers is less than 1024 pixels.

It is an aim of the present invention to provide spectrometer apparatus which has the capability of providing a higher resolution over a wider spectral range

than the above mentioned linear detector array dispersion spectrometers and the Fourier transform spectrometers.

Accordingly, in one non-limiting embodiment of the present invention there is provided spectrometer apparatus comprising a dispersive spectrometer which operates to disperse an incoming spectrum into a plurality of spectral bands extending in a first direction, a Fourier transform spectrometer which generates in a second direction an interferogram of each of the spectral bands, and a two-dimensional detector array.

Usually the first and the second directions will be at right angles to each other.

The spectrometer apparatus of the present invention is such that the dispersive spectrometer and the Fourier transform spectrometer generate information across the two dimensional detector array, thereby making use of a much larger number of pixels than is possible with a spectrometer using a linear detector array. This greater amount of information is able to provide the required high resolution over a wide spectral range. In some cases, some capacity may still be left for providing spatially resolved measurements of the source.

The spectrometer apparatus may include an array of slots in front of the two dimensional array.

Embodiments of the invention will now be described solely by way of example and with reference to the accompanying drawings in which:

Figure 1 shows a dispersive spectrometer;

Figure 2 shows a Fourier transform spectrometer;

Figure 3 shows a two dimensional detector array high resolution spectrometer;

Figure 4 shows a detector array;

Figure 5 shows a detector array illustrating "binning" rows to increase throughput at reduced resolution;

Figure 6 shows how an array of parallel entrance slits give spatial resolution of an object field in a first direction;

Figure 7 shows schematically a silica prism spectrometer;

Figure 8 shows dispersion;

Figure 9 shows a Fourier optic;

Figure 10 shows a silica Sagnac interferometer;

Figure 11 shows results obtainable from a silica prism 1 rad angle 2-D spectrometer;

Figure 12 shows results obtainable from a zinc selenide prism 0.75 rad angle 2-D spectrometer;

Figure 13 shows schematically a system generating 2-D spatially resolved spectra of source;

Figure 14 shows schematically an imaging system in a first direction; and

Figure 15 shows a plot of sinc(x) against x.

Referring to Figure 1, a well known linear detector array dispersion spectrometer will first be described. More specifically, consider a 3 dimensional space described by orthogonal cartesian axes x, y, z. Radiation from a source travelling in direction z enters the spectrometer through an entrance slit which is aligned with the direction y and lies in the x,y plane. The entrance slit is then imaged via a dispersing element (normally a grating or a prism) onto a linear detector array. The dispersing element displaces the image of the slit in the x direction by a distance that depends on the wavelength of the radiation in the image. Thus different elements of the linear detector array measure the quantity of radiation in the source over a particular spectral range, defined by the width of the entrance slit (in the direction x), the position and width of the detector element (in the direction x) and the dispersive power of the dispersive element. Radiation from different heights of the entrance slit (in the y direction) are imaged at different heights at the detector array. This makes it possible to use a 2 dimensional detector array to provide spatial resolution of the source in one direction, the y direction.

Advantages of the linear detector array dispersing spectrometer (Over a scanning spectrometer)

1. Radiation is measured at all wavelengths at the same time.
2. The spectrometer has no moving parts.
3. 1 dimensional spatial resolution of the source is achievable with a 2 dimensional detector array.

Disadvantages of the linear detector array dispersing spectrometer

1. Resolution is limited by the number of elements in the detector array in the x direction, typically no more than 1024 detectors. This means that if the spectrometer is set to cover a spectral range λ_1 to λ_2, the best spectral resolution achievable is $\Delta\lambda = (\lambda_2 - \lambda_1)/1024$. $\Delta\lambda$ can only be decreased by decreasing $(\lambda_2 - \lambda_1)$.
2. Grating dispersion elements generate a number of diffracted orders which must be separated using order sorting filters.
3. Single dispersive element system that is likely to have poor stray light performance.
4. Detector arrays have a limited dynamic range, typically less than 10^5.

5. The entrance slit limits the source size that can be accepted. The entrance slit width sets the highest resolution that is achievable. Increasing the entrance slit width increases the radiation input but at the expense of resolution. Slit height is, in principle, only limited by the height of the detector array elements.

A well known linear detector array Sagnac interferometer Fourier transform spectrometer will now be considered with reference to Figure 2.

Radiation travelling from a source in direction z enters the Sagnac Interferometer through an entrance aperture lying in the x,y plane. This aperture is then imaged in the y direction through the Sagnac interferometer to form two separated images of the entrance aperture, separation being in the y direction. (The Sagnac interferometer also changes the direction of propagation of the radiation in the y,z plane but, for this discussion, notation of direction will continue to be made against the propagation direction which will continue to be referred to as the z direction. This will be made clear by referring to Figure 2.)

A Fourier optic is then positioned so that the separated images focused in the y direction lie at its focal point. This collimates the radiation from the two images to form two interfering plane waves. Each of these

plane waves has constant phase in the x direction. However the phase difference between the plane waves varies linearly in the y direction, so the waves interfere to produce an interferogram in the y direction. This falls on the detector array and is recorded. The data is subsequently processed by taking the Fourier transform to generate the spectrum of the source. It is normal practice to add a cylindrical lens to the system to bring radiation to a focus in the x direction at the detector array. This increases the intensity on the detector array which has a limited extent in the x direction.

The Fourier transform process to generate a spectrum from an interferogram is well known. If the intensity of the interferogram I (δ) is recorded as a function of path difference δ between the two plane waves, then

$$I(\delta) = 2\int_0^{\infty} L(k)\cos(2\pi\delta k)\,dk$$

where L(k) is the spectrum of the source being measured, at wavenumber k

and the Fourier transform generates:

$$L(k) = 2\int_0^{\infty} I(\delta)\cos(2\pi\delta k)\,d\delta$$

Hence the measurement of I(δ) can be used to calculate L(k).

For a spatially modulated Fourier transform interferometer each detector element in the array has a finite width and hence records the interferogram over a finite path difference δ_1 to δ_2 or $\Delta\delta$.

Hence
$$\int_{\Delta\delta} I(\delta)\, d\delta = \int_{\Delta\delta} 2 \int_0^{\infty} L(k) \cos(2\pi\delta k)\, dk\, d\delta$$
$$I(\delta_p) = 2 \int_0^{\infty} \frac{L(k)\sin(\pi\, \Delta\delta\, k)}{\pi\, k\, \Delta\delta} \cos(2\pi\, \delta_p\, k)\, dk$$

where δ_p = mean path difference across each pixel $(\delta_1 + \delta_2)/2$

and
$$\frac{L(k)\sin(\pi\, \Delta\delta\, k)}{\pi\, \Delta\delta\, k} = 2 \int_0^{\infty} I(\delta_p) \cos(2\pi\, \delta_p\, k)\, d\delta_p$$

and hence L(k) can still be recovered.

However sinc(x) = sin(x) / x is a function that goes to zero at x = π, i.e. $\Delta\delta$ k = an integer, h; and the repeating peaks reduce at 1 / (πh), see Figure 15. These properties of sinc(x) mean that the function L(k) cannot be recovered at $\Delta\delta$ k = an integer and the signal to noise of the recovered L(k) will decrease as $\Delta\delta$ k increases.

In addition the full integral over path difference cannot be calculated, only a sum at equally spaced path differences (this assumes the detector array is uniformly spaced). In this case
$$\frac{L(k)\sin(\pi\, \Delta\delta\, k)}{\pi\, \Delta\delta\, k} = 2 \sum_{p=1}^{n} I(\delta_p) \cos(2\pi\, \delta_p\, k)$$

Again this process is well known and requires the number of path differences summed, n, to be at least twice the number of spectrally resolved points. This process of Fourier transform inversion relies critically on the accuracy of the spacing of the measured points in path difference δp, and in the constancy of $\Delta\delta$ for each pixel of the array. To ensure that this is accurately maintained it may be necessary to add a precisely

manufactured mask with equally spaced slots of equal width in front of each pixel of the detector array. This has the disadvantage of reducing the signal recorded by the ratio of the pixel width to slot width, but has the advantage of reducing for each pixel and hence increasing the value of sinc(x) in the Fourier transform inversion process.

Radiation from different positions from the source in the x direction are imaged at different positions in the x direction (heights) on the detector array. This makes it possible to use a 2 dimensional detector array to provide spatial resolution of the source in one direction, the x direction.

Advantages of the Linear Detector Array Sagnac Interferometer Fourier Transform Spectrometer

1. Radiation is measured at all path differences at the same time, which is important when measuring a time varying course.
2. Each detector records radiation at all wavelengths at the same time, often called the Felgett advantage.
3. No moving parts.
4. In principle, there is no limit to the size of the entrance aperture. In practice, the dimension in the x direction will be limited by the height of the detector elements in the array and limited in the y

direction by the dimensions of the interferometer in the y direction.

5. 1 dimensional spatial resolution of the source is achievable with a 2 dimensional detector array.
6. Very wide spectral range can be covered, limited only by the spectral response range of the detector array and the transmittance/reflectance properties of the material used in the construction of the interferometer.

Disadvantages of the Linear Detector Array Sagnac Interferometer Fourier Transform Spectrometer

(Over a scanning interferometer)

1. The resolution is limited by the number of elements in the detector array in the y direction, typically no more than 1024. The Fourier transform process requires at least 2N data points to achieve a resolving power of 1/N. This means that, if the spectrometer is set to cover the spectral range λ_1 to λ_2 , then the best resolution that can achieved is $\Delta\lambda = (\lambda_2 - \lambda_1)/512$. $\Delta\lambda$ can only be decreased by decreasing ($\lambda_2 - \lambda_1$).
2. Detector arrays have a limited dynamic range, typically less than 10^5. As $\lambda_2 - \lambda_1$ increases, fringe visibility decreases for the same resolution.

This means that the limited dynamic range may limit the resolution achievable.

3. Chromatic dispersion is likely to be present in the interferometer which may be difficult to overcome. This may limit $\lambda_2 - \lambda_1$ that can be covered.
4. The maximum path difference that can be achieved in the Sagnac interferometer is limited by clipping of the beam by the beam splitter. This limits the maximum resolution that can be achieved.
5. Each pixel records a range of path differences ΔS. (A scanning interferometer can measure the interferogram at a set path difference.) This reduces the visibility of the fringes, an effect that becomes more severe as $\lambda_2 - \lambda_1$ increases.

Spectrometer apparatus of the present invention and in the form of a 2 dimensional detector array high resolution spectrometer will now be described with reference to Figure 3. As shown in Figure 3, a dispersive spectrometer and a Sagnac interferometer Fourier transform spectrometer are combined with a 2 dimensional detector array such that the dispersion of the dispersive spectrometer is in the x direction and the interferogram of the interferometer is in the y direction, to form an instrument that maintains most of the advantages of the

individual spectrometers, whilst greatly increasing the resolving power and with some other advantages.

The way in which the higher resolution is achieved can be understood by considering the radiation falling on the detector array, which has m rows in the y direction and n columns in the x direction. The dispersing element spectrometer images a spectrally dispersed image of the entrance onto the detector array so that each of the n columns records the complete spectrum but each of the m rows only covers a small part of the spectrum, $\Delta\lambda$. The interferometer spectrometer generates an interferogram of n points on each of the m rows of the detector array (see Figure 4). However, each row only covers a small fraction of the full spectral range of the input radiation $\Delta\lambda$ and so the interferogram increases the resolution to $\delta\lambda = 2\Delta\lambda/n$. The resolution of the instrument for a 1024x1024 detector array is therefore, typically, improved by a factor of 500 over what can be achieved with each of the instruments used on its own, whilst maintaining the following advantages.

1. Radiation is measured at all wavelengths at the same time.
2. Part of the Felgett advantage is maintained as all the detectors in each row record all the radiation over the wavelength range $\Delta\lambda$ at the same time whilst achieving a resolution of $\delta\lambda$.

3. No moving parts.
4. For measurements in the infrared, only thermal background radiation over the wavelength range $\Delta\lambda$ is included in each interferogram. This may significantly improve the signal to noise ratio for some parts of the spectrum, over that which would occur for a scanning interferometer.
5. 1 dimensional spatial resolution of the source can be achieved if some of the additional resolution is sacrificed, using an array of parallel entrance slits (see below). In practice, when making measurements in the infrared, resolution may be limited by the maximum path difference that can be achieved in the interferometer. In this case, the system can be optimised to provide the best compromise between spatial resolution and spectral resolution.
6. A very wide spectral range can be covered, limited only by the spectral response range of the detector array and the transmittance/reflectance properties of the materials that make up the interferometer. The significant improvement in spectral resolution means that high resolution can be maintained even for a wide spectral coverage, which is not possible with either of the component spectrometers used individually.

In addition, some of the disadvantages of the linear array interferometer spectrometer are reduced.

1. The narrower spectral range for each interferogram increases the visibility of the fringes, reducing the demands on the dynamic range of the detector array.
2. The narrower spectral range for each interferogram reduces the problems related to chromatic dispersion.

The size of the entrance aperture is to some extent constrained in the combination forming the spectrometer apparatus of the present invention. It must be a slit and, for the highest resolution, be of a width similar to that of the width of a detector element. However, if some of the resolution is sacrificed, a wider entrance slit can be used. In this case it is appropriate to add the interferograms of a number of adjacent rows that together have approximately the same width as the entrance slit. This can be done by a process called binning for a CCD array without increasing the readout noise. If s rows are summed for each interferogram, then the interferogram now covers the spectral range $s\Delta\lambda$ and the resolution is reduced to $s\delta\lambda$ (see Figure 5). This process can be carried out by a simple adjustment of the spectrometer apparatus and is equivalent to opening the entrance and exit slit of a monochromator to increase its throughput at the expense of resolution. Typically it will increase the

throughput by the increase of the slit width to the power of two.

The higher resolution that is possible with this configuration is achieved in part by increasing the maximum path difference used to generate the interferogram. This in turn increases the path difference $\Delta\delta$ across each pixel of the array. This reduces the visibility of the fringes, as discussed above. A mask of narrow slots placed in front of the detector array may be used to overcome this problem. This will decrease the signal level recorded but increase the visibility of the fringes.

The height of the entrance aperture (slit) is only limited by the y dimension of the interferometer and detector array, and possibly the y dimension of the dispersive spectrometer.

Spectral Resolution and Spectral Range

Typically 2 dimensional detector arrays are made with 256x256, 512x512 or 1024x1024 detector elements. If one considers the 1024x1024 array, this contains more than a million detectors. Remembering that the Fourier transform process requires at least twice as many measurement points at different path differences for each spectrally resolved point, this implies that a 1024x1024 detector array can resolve a spectrum into up to 500,000 spectrally resolved

points. These points will be equally spaced in wavenumbers in about a thousand overlapping spectra.

Also the maximum spectral resolution of an interferogram is limited to (1/the maximum path difference generated in the interferometer). Typically the maximum path difference that can be achieved for a Sagnac interferometer is likely to be about 15 mm. This limits the spectral resolution to about 0.6 cm^{-1}. Taken together with the number of resolvable points, this indicates that a spectral range of up to 3×10^5 cm^{-1} can be covered with a resolution of 0.6 cm^{-1}. Practical considerations probably more realistically limit this to 4×10^4 cm^{-1}, which is sufficient to cover the whole spectral range of the response of a silicon CCD detector array 200 nm to 1000 nm (5×10^4 cm^{-1} to 10^4 cm^{-1}) with a resolution of 0.0024 nm at 200 nm and 0.06 nm at 1000 nm.

However, for a 1024 x 1024 array the path difference across each pixel $\Delta\delta$ will be 15 mm divided by 1024 or about 15 μm. At 200 nm, 5×10^4 cm^{-1}, this gives $\Delta\delta.k$ = 75, i.e. the fringes are almost completely averaged out across each pixel. To resolve the fringes of the interferogram will require a mask of slots to be placed in front of the detector array, the slots to have a slot width of approximately 1/60 of the pixel width, at the same spacing as pixel width. This may mean that a 15 mm path difference and 0.6 cm^{-1} resolution is not achievable

at 200 nm. A lower resolution could be chosen which will leave some redundancy of pixels in the detector array, and make possible a wider entrance slit to the dispersion spectrometer and/or spatial resolution of the source, see below description for infrared detector array.

For the infrared, less detector elements are required to achieve the maximum resolution possible with a maximum 15 mm path difference. For example at 5μm wavelength, 2 x 10^3 cm^{-1}, only 3 x 10^3 measurement points are required, or only a few rows of the detector array. The redundant rows can be used in two ways, or a combination of the two ways as follows.

1. To increase the entrance aperture slit width and sum the output of adjacent detector rows in the array, and hence the throughput of the spectrometer apparatus.
2. To provide spatial resolution of the source.

1. has been discussed above and is shown in Figure 5.

2. is achieved by using an array of parallel entrance slits, each forming a non-overlapping spectrum on the detector array, each from a different part of the source (see Figure 6). To achieve this the dispersing element must not produce higher order spectra, and so a grating dispersing element cannot be used. A prism would be suitable.

For an instrument working in the infrared spectral region, a cooled entrance aperture and stray light screen would be used to reduce background thermal radiation, see Figure 3.

In order to facilitate a full understanding of the invention, reference will now be made to the following Examples.

Example 1: Silica monolithic interferometer using a 1024x1024 pixel CCD silicon diode array.

The silicon diode array sets the maximum operational wavelength range of this system to 200 nm to 1000 nm (10^4 cm^{-1} to $5 \times 10^4 cm^{-1}$).

The dispersive spectrometer could be either a grating or prism instrument. This example uses a prism because:

(i) only relatively low dispersion is required;

(ii) the prism gives higher throughput over a wider spectral range;

(iii) there is no requirement for order sorting filters;

(iv) the prism provides higher dispersion at shorter wavelengths whilst the grating has constant dispersion at all wavelengths. This means that for the prism each detector array row which records each interferogram, covers approximately the same number of wavenumbers. This makes it possible to set up the spectrometer apparatus so that the highest resolution

achievable (defined by the maximum path difference of the interferometer) can be approximately maintained over the whole spectral range, see Figure 11.

Figure 7 shows the prism spectrometer set up using a silica prism with a prism angle of 1 radian. From Figure 8: $x_\lambda = f_t \, d_\lambda$

where x_λ is the position in the image plane of radiation with wavelength λ , f_t is the focal length of the telescope optic, and d_λ is the dispersion angle at wavelength λ .

Or $s\,p = f_t\,(d_{\lambda'} - d_{1000})$

for the sth of m rows, where p is the pixel size.

Now for the typical CCD array: p = 12 μm, the total number of pixel rows m is 1024, and the range of dispersion angles is:

$d_{200} - d_{1000} = 0.1385$ rads = 7.9^o

For prism angle A = 1 rad, and angle of incidence i = 0.806 rad = 45.175^o

$m.p = f_t(d_{200} - d_{1000})$

$1024 \times 12 \times 10^{-3} = f_t \times 0.1385$, and

$f_t = 89$ mm

Figure 11 plots the wavenumber against pixel row number confirming that each row covers approximately an equal wavenumber range, i.e. approximately 40 cm^{-1}.

A monolithic Sagnac interferometer constructed in silica is assumed. The full acceptance angle of this interferometer is

$$\Theta = 2 \sin^{-1}(n \sin(\tan^{-1}(1 / 8 \sqrt{3})))$$

where n is the refractive index of the interferometer material. For silica

$$\Theta = 0.21 \text{ rad} = 12^{o}$$

Let the image separation by this interferometer be 2y and let the collimating Fourier optic have focal length f_f. Then from Figure 9, the maximum path difference

$$\delta_m = 4 \phi D = 4 D \tan^{-1}(y/f_f)$$

where $\theta = 2 \tan^{-1}(D/f_f)$ and $\phi = \tan^{-1}(y/f_f)$

If $y > f_f$, i.e. the image separation is less than the focal length of the Fourier optic

$$\delta_m \approx 4 D y / f_f \text{ (within 20\% for } y \leq f_f)$$

Now $\tan(\Theta/2) = D / f_f$ and as $\Theta/2 \ll 1$

$\Theta \approx 2 D / f_f \approx 0.21$ Therefore $\delta_m \approx 0.42$ y.

If set δ_m = 15 mm, this gives $y \approx 35.7$ mm and image separation as 71.4 mm. If the images are not to clip the interferometer then the dimension w in Figure 10 (the entrance aperture width of the interferometer) must be larger than this separation. Therefore set w = 75 mm, then the dimension of the interferometer $a - w\sqrt{3} = 130$ mm, see Figure 10.

Now if the detector array is to collect all the interferogram 2D must equal the length of a detector row,

i.e. 1024 x 12 x 10^{-3} mm, i.e. 12.288 mm. From Figure 9, this sets

f_f = 12.288 / 0.21 mm = 58.5 mm.

If the Fourier optic is not to clip the beam it must have a diameter of at least 2D + 2y, i.e. greater than 83.4 mm. This Fourier optic will need to be of high optical quality to ensure a well collimated beam without distortion of the wavefronts. A diamond turned mirror is suitable. A cylindrical mirror of focal length f_x is added to bring the image to a focus in the x direction at the detector array, see Figure 10.

It is necessary to couple the dispersive spectrometer to the interferometer. This requires the focal length of the telescope f_t to be increased so that the image of the dispersed spectrum falls at the exit aperture of the interferometer silica block. This will magnify the image. This will be compensated by the demagnification of the image in the x direction by the ratio of the cylindrical lens focal length f_x to the Fourier optic focal length f_f. This is shown in Figure 14.

Each interferogram covers approximately 40 cm^{-1}. Each row has 1024 pixels. If the Fourier transform achieves 250 resolvable points (the maximum theoretically possible is 512), the resolving power limit of the interferometer will be 0.16 cm^{-1}. However, in practice there will need to be some spectral overlap between

interferograms. For example the entrance slit of the dispersive spectrometer might be set at twice the pixel size, i.e. $24 \mu m$. This will give a slit function of total width of three times $40\ cm^{-1}$, or $120\ cm^{-1}$, and hence a resolving power of $0.48\ cm^{-1}$. This is close to the resolving power limit set by the maximum path difference δ_m of 15 mm, i.e. $1 / \delta_m = 0.6\ cm^{-1}$.

In order to achieve this resolution requires $\Delta\delta .k$ to be less than about one, i.e. $\Delta\delta < 0.2 \mu m$ for radiation of wavelength 200 nm, the worst case. This requires a mask in front of the pixel array of width approximately 1 / 60 of the pixel width. This may be difficult to achieve in practice and it may be appropriate to establish a compromise between resolution and signal strength. Lower resolution will release pixels which can be used to increase the area of the source sampled by the spectrometer apparatus, increasing the signal strength further.

All the optics described above, except for the Fourier optic in Figure 10, have been drawn for clarity as lenses. In practice this will give rise to unacceptable chromatic dispersion. Off-axis mirror optics would be necessary to cover the full spectral range.

Example 2: Zinc Selenide monolithic interferometer using 256x256 InSb (Indium Antimonide) detector array cooled to liquid nitrogen temperature.

The InSb detector array sets the maximum operational wavelength range to 1 μm to about 6 μm (1.67 x 10^3 to 10^4 cm $^{-1}$).

A Zinc Selenide prism, rather than a grating, is chosen for the dispersive spectrometer for the same reasons as in Example 1. In this case, because ZnSe has a higher refractive index than silica, a prism angle of 0.75 rad is chosen. Again

$$s\ p = f_t\ d_\lambda$$

but now p is typically 50 μm and the number of pixel rows m will be 256. The dispersive angles with ZnSe are given by

$$d_1 - d_6 = 0.107 \text{ rad} = 6.1^\circ$$

and for prism angle A = 0.75 rad, chosen angle of incidence i = 1.12 rad = 64.19°.

Therefore $m\ p = f_t\ (d_1 - d_6)$

$$256 \times 50 \times 10^{-3} = f_t \times 0.107, \text{ and}$$

$$f_t = 120 \text{ mm}$$

Figure 12 shows a plot of wavenumber against pixel row number and confirms that each row covers approximately an equal wavenumber range, i.e. 32.6 cm^{-1}.

In this case, because the refractive index of ZnSe is higher than silica, the full acceptance angle of the

interferometer is increased to 0.35 rad. Following similar calculations to those worked in Example 1 gives:

$2\ d\ /\ f_f = 0.35$, and

$\delta_m = 0.7\ y$

Again selecting $\delta_m = 15$ mm gives $y = 21.4$ mm.

This sets $w \approx 45$ mm and $a \approx 78$ mm.

Again 2D should be the length of a detector row, i.e.

$256 \times 50 \times 10^{-3} = 12.8$ mm.

This sets $f_f = 12.8\ /\ 0.35 = 36.6$ mm, and

Fourier optic diameter = 2D + 2y = 12.8 + 42.8 = 55.6 mm.

Each interferogram covers approximately 32.6 cm^{-1}. Each row has 256 pixels. If the Fourier transform achieves 64 resolvable points, the resolving power limit will be 0.5 cm^{-1}. As in Example 1, this is likely to be degraded to about 1.5 cm^{-1} to achieve spectral overlap between interferograms. This resolving power is close to the resolving power set by the maximum path difference δ_m of 15 mm, i.e. $1\ /\ \delta_m = 0.6\ cm^{-1}$.

In order to achieve this resolution requires $\Delta\delta.k$ to be less than about one, i.e. $\Delta\delta < 1\mu m$. For a 256 element detector row, this requires a mask in front of each pixel in the array, of width approximately 1 / 60 of each pixel width.

Example 3: Zinc Selenide monolithic interferometer using 1024 x 1024 PtSi (platinum silicilide) detector array cooled to liquid nitrogen temperature.

The PtSi detector array sets the maximum operational wavelength range to 1 μm to 5 μm (2×10^3 cm^{-1} to 10^4 cm^{-1}). A similar system is established as described in Examples 1 and 2. However, in this case only 64 interferograms of 1024 points are required to cover the spectral range and achieve a resolution of about 0.6 cm^{-1}. Higher resolution is not readily achievable because of the limit of path difference set by the interferometer design. This redundancy makes it possible to set up 16 parallel slits at the entrance of the dispersive spectrometer. The source is imaged onto the parallel slits such that each slit isolates a different part of the image of the source. The processed interferograms then provide 16 spectra from different spatial positions of the source. A suitable scanning optic (e.g. a spinning mirror similar that which is well known for thermal imagers using linear detector arrays to generate a 2-D image of a scene) can be added to sweep the 16 slits across the source image, scanning parallel to the slit length, see Figure 13. If the processing of the interferograms is time sequenced, synchronised with the scanning optic, and processing is carried out a number of times for each scan of the source (for example 16 times per scan), a 2-D spatially resolved

and spectrally resolved image of the source can be generated.

In order to achieve this resolution requires $\Delta\delta.k$ to be less than about one. For a 1024 element detector row, this requires a mask in front of each pixel of the array of approximately 1 / 15 of the pixel width. Arrays with rows of 2048 pixels have been made, which would reduce the slot width to only 1 / 8 of the pixel width. Larger arrays may be available in the future.

It is to be appreciated that the embodiments of the invention described above with reference to the accompanying drawings have been given by way of example only and that modifications may be effected.

CLAIMS

1. Spectrometer apparatus comprising a dispersive spectrometer which operates to disperse an incoming spectrum into a plurality of spectral bands extending in a first direction, a Fourier transform spectrometer which generates in a second direction an interferogram of each of the spectral bands, and a 2-dimensional detector array.

2. Spectrometer apparatus according to claim 1 in which the first and the second directions are at right angles to each other.

3. Spectrometer apparatus according to claim 1 or claim 2 and including an array of slots in front of the 2-dimensional detector array.

4. Spectrometer apparatus according to claim 1 and substantially as herein described with reference to the accompanying drawings.

The Patent Office

Application No:	GB 9619690.2	**Examiner:**	C. R. Brain.
Claims searched:	all	**Date of search:**	14 January 1998

Patents Act 1977
Search Report under Section 17

Databases searched:

UK Patent Office collections, including GB, EP, WO & US patent specifications, in:

UK Cl (Ed.P): G1A (ACDT, AHSL)

Int Cl (Ed.6): G01J 3/45, 3/453

Other: Online: WPI

Documents considered to be relevant:

Category	Identity of document and relevant passage	Relevant to claims
	none	

X Document indicating lack of novelty or inventive step	A Document indicating technological background and/or state of the art.
Y Document indicating lack of inventive step if combined with one or more other documents of same category.	P Document published on or after the declared priority date but before the filing date of this invention.
& Member of the same patent family	E Patent document published on or after, but with priority date earlier than, the filing date of this application.